J Biol Chem. Author manuscript; available in PMC 2011 September 22.

Published in final edited form as:
J Biol Chem. 2003 May 02; 278(18): 16159–16168. doi:10.1074/jbc.M213126200.

Association of Kinesin Light Chain with Outer Dense Fibers in a Microtubule-independent Fashion*

Bhupinder Bhullar[‡,§,¶], **Ying Zhang**[‡,§], **Albert Junco**[‡,¶], **Richard Oko**[‖], and **Frans A. van der Hoorn**[‡,**]

[‡]Department of Biochemistry and Molecular Biology, University of Calgary, Calgary, Alberta T2N 4N1, Canada

[‖]Department of Anatomy and Cell Biology, Queen's University, Kingston, Ontario K7L 3N6, Canada

Abstract

Conventional kinesin I motor molecules are heterotetramers consisting of two kinesin light chains (KLCs) and two kinesin heavy chains. The interaction between the heavy and light chains is mediated by the KLC heptad repeat (HR), a leucine zipper-like motif. Kinesins bind to microtubules and are involved in various cellular functions, including transport and cell division. We recently isolated a novel KLC gene, *klc3. klc3* is the only known KLC expressed in post-meiotic male germ cells. A monoclonal anti-KLC3 antibody was developed that, in immunoelectron microscopy, detects KLC3 protein associated with outer dense fibers (ODFs), unique structural components of sperm tails. No significant binding of KLC3 with microtubules was observed with this monoclonal antibody. *In vitro* experiments showed that KLC3-ODF binding occurred in the absence of kinesin heavy chains or microtubules and required the KLC3 HR. ODF1, a major ODF protein, was identified as the KLC3 binding partner. The ODF1 leucine zipper and the KLC3 HR mediated the interaction. These results identify and characterize a novel interaction between a KLC and a non-microtubule macromolecular structure and suggest that KLC3 could play a microtubule-independent role during formation of sperm tails.

Kinesin light chains (KLCs)[1] are components of the conventional kinesin motor molecule that consists of two kinesin heavy chains (KHCs) associated with two KLCs. Kinesins bind to and move along microtubules, powering the transport of proteins, macromolecules, and organelles (reviewed in Refs. 1–5). Although extensive work has been done on elucidating the structure and function of KHCs, relatively little is known about light chains. KLCs have been suggested to bind cargo and to regulate the activity of KHCs. Clues as to possible

*This work was supported in part by grants from the Canadian Institutes of Health Research (to R. O. and F. A. v. d. H.) and from the Natural Sciences and Engineering Council of Canada (to R. O.).

**To whom correspondence should be addressed: Dept. of Biochemistry and Molecular Biology, University of Calgary, 330 Hospital Dr. N. W., Calgary, Alberta T2N 4N1, Canada. Tel.: 403-220-3323; Fax: 403-283-8727; fvdhoorn@ucalgary.ca.
§Both authors contributed equally to this work.
¶Supported in part by a studentship from the Alberta Cancer Foundation.

[1]The abbreviations used are: KLCs, kinesin light chains; KHCs, kinesin heavy chains; HR, heptad repeat; KRPs, kinesin-related proteins; ODFs, outer dense fibers; FS, fibrous sheath; mAbs, monoclonal antibodies; MBP, maltose-binding protein; TBS, Tris-HCl-buffered saline; GST, glutathione *S*-transferase.

functions and the domains involved came from sequence comparisons and genetic analysis of KLCs that were cloned from *Caenorhabditis elegans* (6), sea urchin (7), squid (8), *Drosophila* (9, 10), and mammals (11–16). In mouse, KLC1, a largely neuronal form of KLC, and the ubiquitous KLC2 have been identified (12). KLCs share an N-terminal heptad repeat (HR), reminiscent of a leucine zipper motif, that is involved in binding to KHCs (10, 17). The KLC middle region is highly conserved and consists of tandem tetratricopeptide repeats that, in other proteins, mediate protein interactions (18). Their role in KLC function may be similar. The highly variable C-terminal region of KLCs has been proposed to bind cargo such as organelles and macromolecules; this is supported by direct binding studies in which rat KLC1b was shown to bind to mitochondria (13) and by the use of specific antibodies that bind to KLC and block its interaction with organelles (14). As mentioned, KLCs may also regulate KHC and keep it in an inactive state by preventing the active conformation of KHC (11). This was supported by the recent analysis of KLC1 knockout mice; mutant mice were small and exhibited motor disabilities (19). Also, in these mice, a pool of KHC KIF5A was mislocalized to the peripheral *cis*-Golgi.

We recently reported the isolation of a novel KLC gene, *klc3*, which contains a conserved HR motif that mediates binding to KHCs as well as five tetratricopeptide repeats (20). In association with KHC, KLC3 binds to microtubules in an ATP-dependent manner. KLC3 is expressed in several tissues, including testis and brain; analysis of different male germ cells demonstrated that spermatids are the major site of KLC3 expression. Interestingly, male haploid germ cells do not detectably synthesize KLC1 and KLC2, as determined by reverse transcription-PCR, suggesting that KLC3 probably carries out its function in transport and other motor-based processes and/or that other spermatid KLCs remain to be identified. This is in agreement with the observation that male KLC1 knockout mice are fertile (19). Kinesin-related proteins (KRPs), which do not contain light chains, have also been described in rat testis (21, 22), and two KRPs have sequence similarity to the previously described BimC subfamily of KRPs involved in mitosis (23). The other KRPs expressed in testis had no homology to known kinesins and likely represent novel family members. The KIF3 KRPs were also detected in testis (24); KIF3A and KIF3B form heterodimers that function as microtubule-based (+)-end transporters of membranous organelles (25). A KIF3C knockout mouse is viable and apparently normal (26). Finally, kinesin II, a member of the KIF3 family, is expressed in developing rat, sea urchin, and sand dollar sperm tails (27, 28). Because kinesins and KRPs transport cargo on microtubule tracks, it is interesting that rat testicular KRP2 and KRP6 are associated with spindle microtubules (22). Together, these data suggest that conventional kinesins as well as KRPs play a role in spermatid flagellar transport.

Spermatogenesis is characterized by continuous proliferation and differentiation of germ cells. Upon completion of meiosis, haploid cells called spermatids emerge and differentiate into spermatozoa through a process known as spermiogenesis. Major morphological changes occur at this stage, including nuclear condensation and formation of the sperm tail, which contains unique structures not present in cilia and flagella, *viz.* outer dense fibers (ODFs) and the fibrous sheath (FS). The sperm tail can be subdivided into distinct regions, including the midpiece, which contains all mitochondria surrounding the ODFs and axoneme, and the principal piece, which contains the FS, ODFs, and axoneme. Several ODF components and

associated proteins were recently cloned, and we demonstrated that they interact specifically via leucine zipper motifs (29–31). The function of ODFs remains unknown, but might be manyfold, including strengthening of the long sperm tail, a function in elastic recoil; linking of the FS and mitochondrial sheath to the axoneme; and regulation of motility.

To investigate the localization of KLC3 in developing spermatids, we raised monoclonal and polyclonal antibodies against KLC3. Using the monoclonal antibodies (mAbs), we discovered the association of KLC3 with ODFs in elongating spermatids, a structure devoid of microtubules, and details of this association were explored. The molecular basis of the ODF association is the ability of KLC3 to bind to the major ODF protein ODF1.

EXPERIMENTAL PROCEDURES

Antibody Production and Immunocytochemical Analysis of KLC3 Expression in Testis

A fusion protein containing maltose-binding protein (MBP) linked to KLC3 (20) was produced by inducing transfected TB1 bacteria with isopropyl-β-D-thiogalactopyranoside as described (29). Bacteria were lysed by sonication. After centrifugation, the MBP-KLC3 fusion protein was purified from the bacterial extract using amylose-agarose columns and eluted using maltose. Eluted fusion protein was analyzed by SDS-PAGE. For mAb production, 6-week-old BALB/c mice were injected with 10 μg of MBP-KLC3 fusion protein. For hybridoma production, SP2/MIL-6 myeloma cells (grown in Dulbecco's modified Eagle's medium supplemented with 10% fetal calf serum) were fused to spleen cells. mAb production was analyzed by immunofluorescence using frozen rat testicular sections and Western blot assays using NitroPlus membranes (Micron Separations Inc., Westboro, MA) onto which MBP-KLC3 had been transferred. Polyclonal antibodies were produced as follows. New Zealand White rabbits were injected with purified MBP-KLC3, initially with complete Freund's adjuvant and subsequent injections with incomplete Freund's adjuvant. Serum was collected and tested for KLC3 recognition by Western blot analysis as described above. Affinity-purified polyclonal anti-KLC3 antibody was isolated as described (30) by incubation of total antibodies with membrane-immobilized MBP-KLC3 protein, washing of membrane strips, and elution of bound antibodies.

Adult male Sprague-Dawley rats were anesthetized, and their testes and epididymides were fixed by retrograde perfusion through the abdominal aortas either with standard Bouin's fixative for histology or with 0.8% glutaraldehyde and 4% paraformaldehyde in 0.1 M phosphate-buffered saline containing 50 mM lysine (pH 7.4) for ultrastructure. After perfusion, the tissue designated for electron microscopy was razor-cut into 1-mm^2 blocks, immersed in the respective fixative for 1 h, washed extensively with buffer, and processed for Lowicryl embedding. The issue designated for light microscopy was razor-cut into 3–4-cm^2 blocks, immersed in Bouin's fixative overnight, washed several times over 1 day with 70% ethanol, and processed for paraffin embedding.

Immunohistochemistry—After an extensive wash with 70% ethanol, the tissue blocks were dehydrated and embedded in paraffin by standard procedures. Five-μm sections were deparaffinized, hydrated through a graded series of ethanol concentrations, and immunostained as previously described (32).

Immunoelectron Microscopy—Processing of tissues for Lowicryl K4M embedding followed a standard protocol used in our laboratory (33). Lowicryl-embedded ultrathin sections of testes and epididymides were mounted on 200-mesh Formvar-coated nickel grids, transferred, and floated tissue side down on 10–20-μl drops of the following solutions: 10% goat serum in 20 mM Tris-HCl-buffered saline (TBS) (pH 7.4), 15 min; anti-KLC3 mAb diluted 1:10 in TBS, 1 h; TBS containing 0.1% Tween 20, 5 × 5 min; 10% goat serum in TBS, 15 min; colloidal gold (10 nm)-conjugated goat anti-mouse IgG diluted 1:20 in TBS, 45 min; TBS containing Tween 20, 3 × 5 min; and distilled H_2O, 2 × 5 min. The sections were then counterstained with uranyl acetate and lead citrate and examined by electron microscopy. Controls consisted of replacing the primary antibody (anti-KLC3) step with TBS or mAbs raised against other proteins that were diluted 1:10 in TBS.

KLC3 and ODF1 Plasmid Constructs

The KLC3 C-terminal deletion (KLC3ΔC) was created by PCR using forward primer C1478 (5′-CGCTAAGTGGACTGGCTGCAG-3′), reverse primer C1174 (5′-GCTGAGGATCTCCTTGTATAGCTCC-3′), and pB-S(ATG)KLC3 (20) as a template. The deletion mutant was cloned into the pGAD424 vector for use in yeast. Wild-type KLC3- and KLC3ΔHR mutant-containing plasmids (20) and all ODF1-containing plasmids (29, 34) have been described previously.

KLC3-ODF Binding Assays

In Vitro KLC3-ODF Binding Assay—ODFs were isolated from rat epididymal spermatozoa as described by Oko (35). Vectors containing KHC, KLC3, and the KLC3ΔHR deletion mutant have been described previously (20). To analyze binding of KLC3 protein to purified ODFs, KLC3, KLC3ΔHR, KLC3Δzip, or KHC was transcribed *in vitro* and translated in the presence of [^{35}S]cysteine using the T_NT reticulocyte transcription and translation system (Promega). Radiolabeled proteins were incubated with purified ODFs at 30 °C for 15 min. ODFs were pelleted at 30,000 rpm for 15 min at 22 °C. Supernatants were saved for SDS-PAGE analysis. Two subsequent washing/pelleting reactions were performed. Aliquots of both supernatants and pellets were boiled in SDS sample buffer and analyzed by electrophoresis on 10% SDS-polyacrylamide gels, and the gels were dried and exposed to Biomax film (Eastman Kodak Co.).

ODF Western Blot Binding Assay—To identify proteins present in purified ODFs or the FS that may bind KLC3, a modified Western blot binding assay was carried out. Proteins from fractionated male germ cells obtained by centrifugal elutriation (36, 37) or from ODFs and the FS were separated on 10–15% gradient SDS-polyacrylamide gels and transferred to NitroPlus membranes. Membranes were blocked and washed as described above and were then incubated in Western blot binding buffer (30) containing 1 mM ATP and 1000 cpm/ml ^{35}S-labeled KLC3 protein, produced by *in vitro* translation, for 16 h at 4 °C. Blots were washed three times and exposed to Biomax film.

Yeast Two-hybrid KLC3 Interaction Assays—The use and construction of yeast two-hybrid plasmids, cDNA expression vectors based on pGAD (containing the GAL4 activating domain) and pGBT9 (containing the Gal4 DNA-binding domain), and cell lines have been

described previously (29). The interaction between KLC3 and ODF1, ODF2, and mutants was analyzed in yeast as described above. Colonies that grew on His^- plates were tested for β-galactosidase expression on membranes as described previously (29).

Western Blot Analysis of Purified ODFs—Extracts prepared from purified ODFs were separated by electrophoresis on SDS-polyacrylamide gels and transferred to Hybond-P polyvinylidene difluoride membranes (Amersham Biosciences). Specific proteins on blots were analyzed by incubation with antisera to ODF1, β-tubulin (Sigma), KHC (Chemicon International, Inc.), and KLC3, followed by horseradish peroxidase-coupled secondary antibodies. Blots were developed using chemiluminescence (LumiGLO chemiluminescent substrate system; Kirkegaard & Perrie Laboratories, Inc., Gaithersburg, MD).

RESULTS

KLC3 Associates with Spermatid ODFs

We recently cloned and characterized a novel gene, *klc3*, which has the distinguishing structural and functional features of KLC proteins (20). Interestingly, we found that spermatids express only KLC3, not the other known light chains KLC1 and KLC2. This suggested that KLC3 might carry out roles specific to the process of spermiogenesis in addition to a general function in transport. To approach this possibility, we generated affinity-purified polyclonal anti-KLC3 antibodies as well as monoclonal anti-KLC3 antibodies (20), both of which specifically recognized the 58-kDa KLC3 protein, as shown in Fig. 1; polyclonal and monoclonal anti-KLC3 antibodies recognized KLC3 in elutriated elongating spermatids (*lanes 1* and *4*, respectively) as well as in epididymal sperm (*lanes 3* and *5*, respectively). No protein was observed in early spermatocytes (*lane 2*) or liver (*lane 6*), which does not produce *klc3* mRNA (20). These antibodies were next used in immunocytochemistry of rat testis. Surprisingly, the polyclonal and monoclonal antibodies displayed overlapping but distinct KLC3 expression patterns during spermiogenesis at the light microscopic level (as shown in Figs. 2 and 3). The results of these studies are summarized in Fig. 4. Note that rat spermiogenesis is divided in 19 distinguishable steps of development.

Fig. 2 shows the results of immunocytochemistry using affinity-purified polyclonal antibodies and illustrates that KLC3 protein expression was first detectable in step 8 round spermatids (stage VIII of the seminiferous epithelium) (*middle* and *lower panels*). KLC3 immunostaining appeared to peak in the cytoplasm of elongating spermatids at stages XIV-I, thereafter gradually diminishing from this region (steps 16–19, stages II–VIII), but at the same time becoming prominent in the tails of maturing elongated spermatids. Note that, initially, KLC3 staining in the tail was light (*arrows*), but later became very dense (*arrowheads*) along the entire tail. This suggests that KLC3 associates with structures that run the length of the tail, *viz.* the axoneme and/or ODFs. Fig. 3 shows the results of immunocytochemical analyses using mAb B11. KLC3 labeling was first detectable in step 14 spermatids (Fig. 3*A*). Cytoplasmic staining became prominent from step 15 spermatids onwards and at later steps became concentrated in the midpiece area of elongated sperm tails (Fig. 3*B*). Fig. 3*C* (and *inset*) shows cross-sections of midpieces, and Fig. 3*D* (and *inset*)

shows longitudinal midpiece sections, both exposures revealing a strong KLC immunoreactivity in mature spermatids to be exfoliated. This result indicates that KLC3 proteins detected by the mAb are present in association with structures present in the sperm tail midpiece (*e.g.* the ODFs and/or mitochondrial sheath), but not the axoneme or FS. The *upper panel* of Fig. 4 summarizes the period of spermatid development showing KLC3 staining as detected by the polyclonal and monoclonal antibodies; the *lower panel* indicates schematically KLC3 staining in the cytoplasm and tail structures observed using the mAb.

Localization of KLC3 to ODF Surfaces

Because KLC3 immunoreactivity appeared concentrated in the midpieces of elongated spermatids, we used the mAb in a more precise ultrastructural analysis of KLC3 localization in spermatid tails. The results shown in Fig. 5 reveal a novel association pattern for KLC3 in mature step 19 elongated spermatids. Fig. 5 (*A* and *B*) shows cross-sections, and Fig. 5*C* shows a longitudinal section through rat sperm. The mAb detected KLC3 predominantly in association with the surface of ODFs, but not with the axoneme, confirming the light microscopic observations with this antibody. The KLC3 immunogold label was observed between adjacent ODFs and between ODFs and surrounding mitochondria (examples are shown in Fig. 5*D*). Quantitation of gold label in all micrographs indicated that labeling was not significant outside of this designated region, including sites within the ODFs, FS, or axoneme. In mature sperm, microtubules have not been shown to be present between adjacent ODFs or between mitochondria and ODFs (38). Based on these results, we conclude that mAb B11 detects KLC3 proteins that display a novel subcellular localization in elongating spermatids, and we proceeded to explore the possibility of a binding association of KLC3 with the macromolecular ODF structure.

The HR of KLC3 Is Involved in ODF Interaction

An *in vitro* ODF binding assay was developed to study the molecular basis of the novel KLC3-ODF association observed in elongating spermatids. In preparation, ODFs were isolated and purified from mature rat epididymal spermatozoa using gradient centrifugations as described (35). Purified ODFs were examined by Western blot analysis to confirm that they were completely devoid of endogenous β-tubulin and KHC, which would have complicated the binding assay interpretations, and we tested them for the presence of KLC3. Fig. 6 shows that purified ODFs did not contain detectable β-tubulin or KHC, indicating that the ODF preparations were not contaminated with axonemal components. In addition, we did not detect KLC3 in purified ODF preparations, indicating that, as suggested by the immunoelectron microscopic data, KLC3 is an ODF-associated protein rather than an integral ODF protein and is lost in the ODF isolation procedures. Controls for all three proteins were positive. Brain expressed KHC; microtubule preparations contained β-tubulin; and testis expressed KLC3, as expected.

Next, *in vitro* translated ^{35}S-radiolabeled KLC3 was added to purified ODFs in the presence of 0.5% Sarkosyl. After binding, ODFs were pelleted through a sucrose cushion, washed and repelleted several times, and analyzed by SDS-PAGE. The results show that wild-type KLC3 (58 kDa) could bind to purified ODFs in the absence of detectable KHC or microtubules (Fig. 7, compare *lanes 1* and *5*), as evidenced by its presence in ODF pellets. To analyze the

specificity of this assay, we next tested binding of an unrelated protein ($p21^{ras}$) to purified ODFs. The Ras oncoprotein failed to bind (compare *lanes 4* and *8*). To further address specificity, we mixed *in vitro* translated radiolabeled KLC3 and KHC proteins and subjected them to ODFs; in comparison with KLC3, KHC showed virtually no binding (*lanes 9* and *10*). We next exploited this binding assay to delineate KLC3 sequences involved in ODF binding; deletion mutants were constructed in the HR and C-terminal regions of KLC3 and analyzed in the ODF binding assay. The results show that the 52-kDa KLC3ΔHR mutant could not bind to ODFs (*lane 6*). Deletion of the variable C-terminal sequence in the 49-kDa KLC3ΔC mutant had no significant effect on ODF binding (compare *lanes 3* and *7*). These results indicate that the HR domain of KLC3 is involved in ODF interaction. This is interesting in light of the fact that the HR mediates KLC-KHC binding in the context of a kinesin complex.

Western Blot Overlays Show Binding of KLC3 to a 27-kDa ODF Protein

ODFs contain several major proteins as well as a number of other integral proteins. We have previously cloned and characterized two major ODF proteins, ODF1 (27 kDa) (39) and ODF2 (84 kDa) (29). To identify which ODF protein(s), if any, bind to KLC3, we carried out Western blot overlay assays using radiolabeled KLC3 as a probe; extracts were prepared from purified spermatocytes and elongating spermatids as well as from isolated purified ODFs and the FS. Note that, whereas elongating spermatids produced ODF and FS proteins, spermatocytes did not. Extracted proteins were separated by SDS-PAGE, transferred to filters, and probed with ^{35}S-radiolabeled wild-type KLC3. We also carried out this assay using the ^{35}S-radiolabeled KLC3ΔHR deletion mutant as a control for non-specific binding because this mutant did not bind ODFs (see Fig. 7). The results of the binding experiments are shown in Fig. 8 (*A* and *B*), and the corresponding Coomassie stains of these gels are also shown (Fig. 8, *C* and *D*). The results show that wild-type KLC3 could bind to a 27-kDa ODF protein present in spermatids (Fig. 8*A*, *lanes 1* and *2*), but not to any proteins from spermatocytes (*lane 3*). Deletion of the HR domain abolished binding to this spermatid protein (Fig. 8*B*, *lanes 6* and *7*). It is also shown that wild-type KLC3 bound specifically to a 27-kDa protein in purified ODFs; the detected band (Fig. 8*A*, *lane 4*) overlapped exactly with the ODF1 protein (Fig. 8*C*, *lane 4*). Together, these results strongly suggest the possibility that KLC3 can bind to the major ODF protein ODF1 (see below). Fig. 8A also shows that KLC3 did not bind to the 84-kDa ODF2 protein (*lane 4*) or to any FS proteins (*lane 5*). These data suggest that ODF1 is a strong candidate for a KLC3-interacting ODF protein and confirmed our observation that the HR domain is involved in KLC3-ODF binding.

Specific KLC3-ODF1 Interaction Is Mediated by Leucine Zipper Motifs

ODF1 is a multifunctional protein that contains an N-terminal leucine zipper motif that specifies binding to several ODF and ODF-associated proteins (29–31) as well as a conserved CGP repeat in the C terminus that we recently showed binds to a novel RING finger protein, OIP1 (40). To prove that ODF1 can bind KLC3 and to delineate regions in ODF1 involved in this binding, we used two different assays: the yeast two-hybrid system and a cell-free GST-ODF1 pull-down assay. In addition, because the HR domain resembles a leucine zipper motif, and because we had demonstrated that the major ODF and ODF-

associated proteins interact using leucine zipper motifs, one possibility was that the KLC3 HR domain interacts with the ODF1 leucine zipper motif.

First, interaction experiments were carried out in yeast using selection for growth in the absence of His and activation of the β-galactosidase reporter gene as indicators of protein interaction. The results of yeast two-hybrid assays are shown in Fig. 9 and Table I. The results obtained in the His^- selection and LacZ activation assays were identical. These data demonstrate that (i) KLC3 can bind to ODF1, but not to ODF2, in agreement with the suggestions from the Western blot overlay assays; (ii) KLC3 associates with the N-terminal half of ODF1 (ODF1NT), but not with the C-terminal half (ODF1CT); and (iii) deletion of the KLC3 HR domain abolishes binding to ODF1, whereas deletion of the KLC3 C terminus does not affect binding. The results also show that the first 100 amino acid residues of ODF1 (ODF1NT100) suffice for KLC3 interaction. In conclusion, the yeast data demonstrate that KLC3 and ODF1 can interact directly.

To confirm and extend the yeast results, we incubated different GST-ODF1 fusion proteins (34) with ^{35}S-radiolabeled KLC3. Bound KLC3 was eluted and analyzed by SDS-PAGE and autoradiography, and binding was quantitated. The results are shown in Fig. 10. Fig. 10*A* shows schematically the GST-linked ODF1 fragments that were used in this analysis as well as the approximate locations of the leucine zipper motif and the CGP repeats. Fig. 10*B* shows a Coomassie-stained gel for quantitation of the amount of GST fusion proteins used in the binding reactions. Fig. 10*C* shows the autoradiogram of bound KLC3. For quantitation of binding results, the bands in Fig. 10*C* were normalized for input GST fusion proteins (shown in Fig. 10*B*). These results show that KLC3 did not bind GST, as expected. KLC3 bound efficiently *in vitro* to the ODF1 N-terminal half, but not to the ODF1 C-terminal half or a deletion variant of the C-terminal half (GST-ODF1ΔCT) that removes most of the CGP repeats, in agreement with the results in yeast. Importantly, deletion of the ODF1 leucine zipper (GST-ODF1NT-(25–147)) significantly decreased KLC3 binding to 5% of wild-type KLC3 binding. The first 100 amino acid residues in the ODF1 N-terminal half (GST-ODF1ΔNT) bound KLC3 with the same efficiency as wild-type KLC3. Together, the binding experiments positively identify ODF1 as the ODF protein that binds KLC3. Moreover, we have shown that this interaction is mediated by the ODF1 leucine zipper motif.

DISCUSSION

Kinesins are heterotetrameric mechanoenzymes that consist of two heavy chains and two light chains (4, 5). They are abundant and have been detected in virtually all cell types. Kinesins bind to and move along microtubules toward the (+)-end with few exceptions, such as the KRP NCD (41). Most work has concentrated on the motor domain-containing KHC proteins, which share motifs with the myosin head (42). The globular motor domain is linked via β-sheets to a coiled-coil tail domain responsible for dimerization. The C terminus of KHC interacts with the HR domain in the N terminus of KLC (43). Because kinesins and KRPs bind microtubules, it was proposed and later demonstrated that they function in movement of organelles associated with axons, the axoneme, and mitotic spindles (44–46). Kinesins and KRPs are also involved in spindle assembly and maintenance, attachment of

microtubules to chromosomes, and chromosome movement (47). In contrast to KHC and KRPs, little is known about the interacting partner of conventional kinesins, KLC. Two roles have been postulated for KLCs.

First, as a component of kinesin, KLCs mediate the interaction between microtubules, kinesin, and membrane surfaces, including vesicles (9), microsomes (48), mitochondria (13), and the *trans*-Golgi network (49). Several experiments support such a role. In *Drosophila* KLC mutants, large aggregates ("organelle jams") accumulate in axons, resulting from a block in axonal transport (9). Also, anti-KLC antibodies inhibit fast axonal transport without affecting microtubule binding or ATPase activity *in vitro* and cause release of purified membrane vesicles from kinesin (14). Rat KLC1b binds via its C terminus to mitochondria in cultured CV1 cells and human skin fibroblasts (13). The divergent C terminus of KLC has been proposed to function as an attachment site for organelles to be transported along microtubules. Second, KLC appears to regulate kinesin activity. Upon binding of KHC to KLC, KHC is released from microtubules and is kept in an inactive state by interaction between the tail and motor domains of KHC. Verhey *et al.* (11) hypothesized that cargo binding triggers a conformational change resulting in microtubule binding of the activated kinesin. As described in the Introduction, several kinesins and KRPs have been detected in sperm, including kinesin associated with the manchette, a transient microtubule structure (50); KRPs (21, 22); kinesin II, a KIF3-based motor molecule (27); and KAP3 (51). It is important to note that kinesin II, which was found in the midpiece, consists of two different KIF3 motor proteins linked to the dynactin component Glued (52, 53) and lacks conventional KLC. From morphogenetic studies, it appears that a flagellar transport mechanism must exist. First, during post-meiotic differentiation of spermatids, a membrane-bound constriction point forms called the annulus, which separates the narrow and long periaxonemal compartment from the bulk of the cytoplasm (*i.e.* cytoplasmic lobe). Proteins needed to form specialized components of the forming sperm tail (*e.g.* the FS and ODFs) must thus pass through the annulus. Second, the FS forms during spermiogenesis in a distal-to-proximal orientation; thus, FS proteins must be transported to the tip of the periaxonemal compartment to begin assembly. The axoneme, which represents the first tail structure to be formed during spermiogenesis, links the periaxonemal compartment with the cytoplasmic lobe through the annulus and thus likely provides the molecular basis for microtubule-based flagellar transport.

KLC3 Protein Can Bind to ODFs

We have reported that the recently discovered kinesin light chain KLC3 can associate with ODFs, one of two unique macromolecular structures in mammalian spermatozoa, the other one being the FS. We discovered, in immunocytochemistry assays using anti-KLC3 mAb B11, that KLC3 protein is present in elongating spermatids from stage XIV onwards and appears to localize to the sperm tail midpiece. Immunoelectron microscopy with the mAb showed that, in mature sperm, KLC3 associates with the surface of ODFs and is present in the space between adjacent ODFs and between mitochondria and ODFs, which are devoid of tubulins (38). KLC3 is not present in the medulla of ODFs, indicating that KLC3 is not an integral ODF protein like ODF1 (36, 54) and ODF2 (29, 55). Indeed, Western blot analysis of highly purified ODFs failed to detect KLC3 (Fig. 6). The same experiment indicated that

KHC is also not an integral ODF protein, and we also showed that KHC has low affinity (if any) for purified ODFs. However, we do not know if KHC is present on ODFs in mature sperm either as part of a kinesin or as an individual protein. Be that as it may, the presence of KLC3 on ODFs occurs in the absence of microtubules. The mAb failed to detect KLC3 label over the axoneme or over the manchette, a microtubule-rich transient structure in elongating spermatids that binds several microtubule-associated proteins (30, 56). We conclude that the monoclonal KLC3 epitope detected in association with the ODFs is not detectable in the association of KLC3 with microtubules in spermatids. Together with our observation that KLC3 can bind *in vitro* to ODFs in the absence of microtubules, these results suggest the possibility that KLC3 may be able to carry out a microtubule-independent role in spermiogenesis (see below).

Leucine Zipper-like Repeats Mediate KLC3-ODF1 Binding

We investigated the mechanism that KLC3 employs to bind to ODFs. First, a new ODF binding assay showed that the HR domain of KLC3 is involved in the ODF association. This is interesting because, in kinesin-based cargo transport, the KLC HR domain interacts with KHC, and cargo associates with the variable KLC C terminus or part of the tetratricopeptide repeats (13, 57). We found that deletion of the C terminus has no effect on ODF binding. Our findings imply that ODFs cannot be categorized as regular cargo for transport. Second, our experiments uncovered that KLC3 binds directly to ODF1 and that it employs its HR sequence in this interaction. Our data predicted that the leucine zipper of ODF1 is involved in KLC3 binding. Indeed, deletion of the ODF1 leucine zipper significantly reduced binding (20-fold) to KLC3. We had previously determined that the ODF1 leucine zipper is crucial for the association with ODF2 (29); SPAG4, a spermatid-specific axoneme-binding protein (30); and SPAG5 (31, 58). The specificity of these leucine zipper-mediated interactions is underscored by our observation that KLC3 does not bind to ODF2 even though ODF2 contains two functional leucine zipper motifs (29, 59).

Role for KLC3 in Organization of Structural Components of the Sperm Tail

Based on the observation that KLC3 is the only one of three known light chains to be expressed in spermatids, we had suggested previously (20) that, in addition to its ability to carry cargo down the sperm tail axoneme in the context of a kinesin-microtubule interaction, KLC3 must fulfill unique spermatid-specific roles. Indeed, the mAb used in this study indicates that KLC3 localizes to ODFs, suggestive of a spermatid-specific role. What is the nature of this binding and what could such a role(s) be?

The results described here suggest the intriguing possibility that KLC3 proteins can bind to spermatid ODFs in a microtubule-independent manner. The data in support of this possibility are the following. (i) The areas surrounding ODFs where KLC3 peptides are detected by mAbs in mature sperm are devoid of microtubules; (ii) the ODF preparations used in the *in vitro* binding assays do not contain β-tubulin; (iii) KLC3 can bind directly to ODF1 in yeast; and (iv) ODF1 and purified ODFs bind to the HR motif in KLC3, a motif normally used for binding KHC to form kinesins, not for interacting with cargo. Occupancy of the KLC3 HR motif by ODF1 will likely exclude KHC from binding to the same sequence. Indeed, preliminary experiments failed to detect a KLC3 complex containing both

ODF1 and KHC (data not shown). Based on these and previous results, we propose that, in spermatids, distinct KLC3KHC · kinesin complexes as well as KLC3·ODF1 complexes exist. The former likely act in paradigm kinesin-mediated cargo transport, whereas the latter may carry out a spermatid-specific function.

A role for KLC3·ODF complexes must take into account the development of major elongating spermatid structures. One intriguing possible role for KLC3·ODF complexes was suggested by the mAb immunocytochemistry experiments. A redistribution of mitochondria from the periphery of spermatids to the axonemal region just below the sperm head, the future midpiece, occurs in step 15–16 spermatids, a developmental stage that coincides with high level expression of KLC3 and a change in localization of KLC3 from a general cytoplasmic one to one in the sperm tail midpiece. In agreement, we observed KLC3 label between ODFs and mitochondria. We found that KLC3 can bind to and cluster mitochondria and that this activity depends on a region different from the HR (data not shown). In the context of a possible role for KLC3 in mitochondrial ODF interactions, the following interesting observation has been made. *hpy* mice, which lack normal axonemal development during spermiogenesis, contain immature spermatids that harbor aggregates of mitochondria clustered around pieces of ODFs (60). This demonstrates that normal axonemal morphogenesis is a prerequisite for tail development, and it also indicates that, in the absence of the axoneme, mitochondria can still redistribute to ODFs. We propose that KLC3 might be involved in aspects of the mitochondrial redistribution.

Acknowledgments

We thank Dr. X. Shao for expert advice on the yeast two-hybrid system and H. Orchard for technical assistance.

References

1. Hirokawa N. Science. 1998; 279:519–526. [PubMed: 9438838]
2. Block SM. Cell. 1998; 93:5–8. [PubMed: 9546384]
3. Moore JD, Endow SA. Bioessays. 1996; 18:207–219. [PubMed: 8867735]
4. Goldstein LS. Trends Cell Biol. 2001; 11:477–482. [PubMed: 11719052]
5. Kamal A, Goldstein LS. Curr Opin Cell Biol. 2002; 14:63–68. [PubMed: 11792546]
6. Fan J, Amos LA. J Mol Biol. 1994; 240:507–512. [PubMed: 8046755]
7. Wedaman KP, Knight AE, Kendrick-Jones J, Scholey JM. J Mol Biol. 1993; 231:155–158. [PubMed: 8496962]
8. Beushausen S, Kladakis A, Jaffe H. DNA Cell Biol. 1993; 12:901–909. [PubMed: 8274223]
9. Gindhart JG Jr, Desai CJ, Beushausen S, Zinn K, Goldstein LS. J Cell Biol. 1998; 141:443–454. [PubMed: 9548722]
10. Gauger AK, Goldstein LS. J Biol Chem. 1993; 268:13657–13666. [PubMed: 8514798]
11. Verhey KJ, Lizotte DL, Abramson T, Barenboim L, Schnapp BJ, Rapoport TA. J Cell Biol. 1998; 143:1053–1066. [PubMed: 9817761]
12. Rahman A, Friedman DS, Goldstein LS. J Biol Chem. 1998; 273:15395–15403. [PubMed: 9624122]
13. Khodjakov A, Lizunova EM, Minin AA, Koonce MP, Gyoeva FK. Mol Biol Cell. 1998; 9:333–343. [PubMed: 9450959]
14. Stenoien DL, Brady ST. Mol Biol Cell. 1997; 8:675–689. [PubMed: 9247647]
15. Cabeza-Arvelaiz Y, Shih LC, Hardman N, Asselbergs F, Bilbe G, Schmitz A, White B, Siciliano MJ, Lachman LB. DNA Cell Biol. 1993; 12:881–892. [PubMed: 8274221]

16. Cyr JL, Pfister KK, Bloom GS, Slaughter CA, Brady ST. Proc Natl Acad Sci U S A. 1991; 88:10114–10118. [PubMed: 1946431]
17. Diefenbach RJ, Mackay JP, Armati PJ, Cunningham AL. Biochemistry. 1998; 37:16663–16670. [PubMed: 9843434]
18. Gindhart JG Jr, Goldstein LS. Trends Biochem Sci. 1996; 21:52–53. [PubMed: 8851660]
19. Rahman A, Kamal A, Roberts EA, Goldstein LS. J Cell Biol. 1999; 146:1277–1288. [PubMed: 10491391]
20. Junco A, Bhullar B, Tarnasky HA, van der Hoorn FA. Biol Reprod. 2001; 64:1320–1330. [PubMed: 11319135]
21. Zou Y, Millette CF, Sperry AO. Biol Reprod. 2002; 66:843–855. [PubMed: 11870094]
22. Sperry AO, Zhao LP. Mol Biol Cell. 1996; 7:289–305. [PubMed: 8688559]
23. Kashina AS, Rogers GC, Scholey JM. Biochim Biophys Acta. 1997; 1357:257–271. [PubMed: 9268050]
24. Nakajima T, Miura I, Kashiwagi A, Nakamura M. Zool Sci. 1997; 14:917–921. [PubMed: 9520632]
25. Yamazaki H, Nakata T, Okada Y, Hirokawa N. J Cell Biol. 1995; 130:1387–1399. [PubMed: 7559760]
26. Yang Z, Roberts EA, Goldstein LS. Mol Cell Biol. 2001; 21:5306–5311. [PubMed: 11463814]
27. Miller MG, Mulholland DJ, Vogl AW. Biol Reprod. 1999; 60:1047–1056. [PubMed: 10084983]
28. Henson JH, Cole DG, Roesener CD, Capuano S, Mendola RJ, Scholey JM. Cell Motil Cytoskeleton. 1997; 38:29–37. [PubMed: 9295139]
29. Shao X, Tarnasky HA, Schalles U, Oko R, van der Hoorn FA. J Biol Chem. 1997; 272:6105–6113. [PubMed: 9045620]
30. Shao X, Tarnasky HA, Lee JP, Oko R, van der Hoorn FA. Dev Biol. 1999; 211:109–123. [PubMed: 10373309]
31. Shao X, Xue J, van der Hoorn FA. Mol Reprod Dev. 2001; 59:410–416. [PubMed: 11468777]
32. Oko R. Andrologia. 1998; 30:193–206. [PubMed: 9739416]
33. Oko RJ, Jando V, Wagner CL, Kistler WS, Hermo LS. Biol Reprod. 1996; 54:1141–1157. [PubMed: 8722637]
34. Shao X, van der Hoorn FA. Biol Reprod. 1996; 55:1343–1350. [PubMed: 8949892]
35. Oko R. Biol Reprod. 1988; 39:169–182. [PubMed: 3207795]
36. Higgy NA, Pastoor T, Renz C, Tarnasky HA, van der Hoorn FA. Biol Reprod. 1994; 50:1357–1366. [PubMed: 7521678]
37. Higgy NA, Zackson SL, van der Hoorn FA. Dev Genet. 1995; 16:190–200. [PubMed: 7736667]
38. Hermo L, Oko R, Hecht NB. Anat Rec. 1991; 229:31–50. [PubMed: 1996783]
39. van der Hoorn FA, Tarnasky HA, Nordeen SK. Dev Biol. 1990; 142:147–154. [PubMed: 1699827]
40. Zarsky HA, Cheng M, van der Hoorn FA. Biol Reprod. 2003; 68:543–552. [PubMed: 12533418]
41. Amos LA, Hirose K. Curr Opin Cell Biol. 1997; 9:4–11. [PubMed: 9013667]
42. Block SM. J Cell Biol. 1998; 140:1281–1284. [PubMed: 9508762]
43. Hackney DD. Annu Rev Physiol. 1996; 58:731–750. [PubMed: 8815818]
44. Diez S, Schief WR, Howard J. Curr Biol. 2002; 19:R203–R205.
45. Hirokawa N, Noda Y, Okada Y. Curr Opin Cell Biol. 1998; 10:60–73. [PubMed: 9484596]
46. Kikkawa M, Sablin EP, Okada Y, Yajima H, Fletterick RJ, Hirokawa N. Nature. 2001; 411:439–445. [PubMed: 11373668]
47. Wilde A, Lizarraga SB, Zhang L, Wiese C, Gliksman NR, Walczak CE, Zheng Y. Nat Cell Biol. 2001; 3:221–227. [PubMed: 11231570]
48. Yu H, Toyoshima I, Steuer ER, Sheetz MP. J Biol Chem. 1992; 267:20457–20464. [PubMed: 1400364]
49. Johnson KJ, Hall ES, Boekelheide K. Eur J Cell Biol. 1996; 69:276–287. [PubMed: 8900492]
50. Hall ES, Eveleth J, Jiang C, Redenbach DM, Boekelheide K. Biol Reprod. 1992; 46:817–828. [PubMed: 1534261]

51. Yamazaki H, Nakata T, Okada Y, Hirokawa N. Proc Natl Acad Sci U S A. 1996; 93:8443–8448. [PubMed: 8710890]
52. Karcher RL, Deacon SW, Gelfand VI. Trends Cell Biol. 2002; 12:21–27. [PubMed: 11854006]
53. Deacon SW, Serpinskaya AS, Vaughan PS, Fanarraga ML, Vernos I, Vaughan KT, Gelfand VI. J Cell Biol. 2003; 160:297–301. [PubMed: 12551954]
54. Morales CR, Oko R, Clermont Y. Mol Reprod Dev. 1994; 37:229–240. [PubMed: 8179907]
55. Schalles U, Shao X, van der Hoorn FA, Oko R. Dev Biol. 1998; 199:250–260. [PubMed: 9698445]
56. Kierszenbaum AL. Mol Reprod Dev. 2001; 59:347–349. [PubMed: 11468770]
57. Gyoeva FK, Bybikova EM, Minin AA. J Cell Sci. 2000; 113:2047–2054. [PubMed: 10806115]
58. Xue J, Tarnasky HA, Rancourt DE, van der Hoorn FA. Mol Cell Biol. 2002; 22:1993–1997. [PubMed: 11884588]
59. Kierszenbaum AL. Mol Reprod Dev. 2002; 61:1–2. [PubMed: 11774369]
60. Bryan JH. Cell Tissue Res. 1977; 180:187–201. [PubMed: 872193]

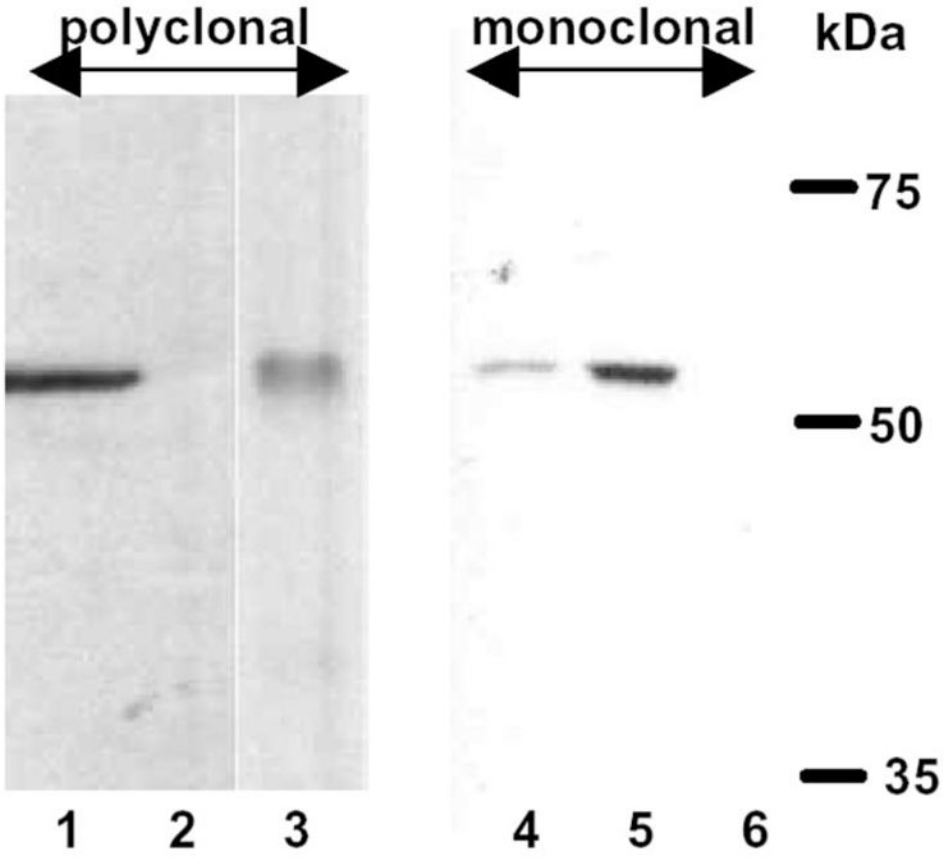

Fig. 1. Specificity of polyclonal and monoclonal anti-KLC3 antibodies

Protein extracts prepared from elutriated rat spermatids (*lanes 1* and *4*), epididymal sperm (*lanes 3* and *5*), spermatocytes (*lane 2*), and liver (*lane 6*) were analyzed by Western blot assays using affinity-purified polyclonal and monoclonal anti-KLC3 antibodies. Note that both antibodies recognized KLC3. Molecular mass markers are indicated to the right.

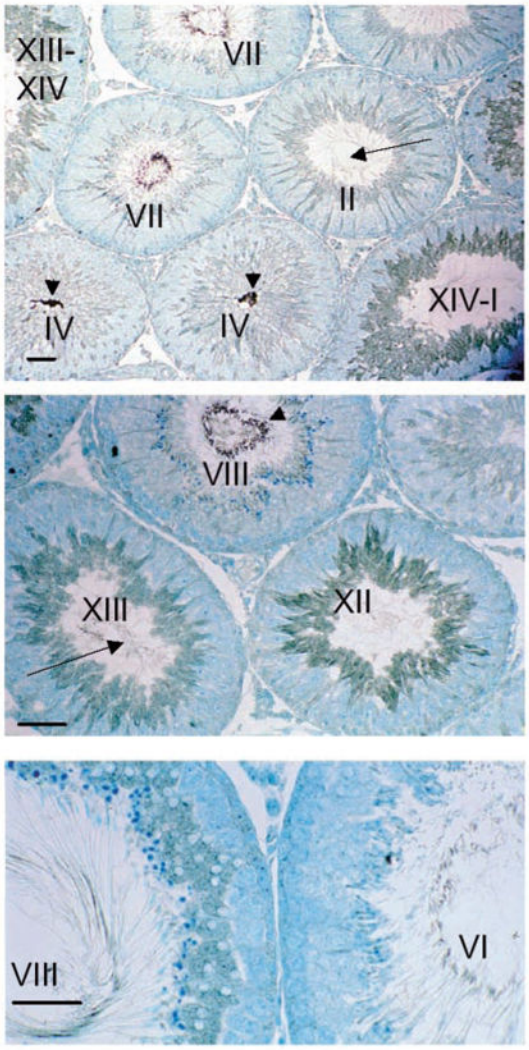

Fig. 2. Immunocytochemistry using polyclonal anti-KLC3 antibodies

Rat testicular sections were prepared, and KLC3 was visualized using affinity-purified polyclonal anti-KLC3 antibodies. Sections were counterstained with methylene blue. The *Roman numerals* refer to the stage of the cycle of the rat seminiferous epithelium of individual cross-sections. Note that KLC3 localized to the cell body of round spermatids at early stages of spermiogenesis and to the forming sperm tail at later stages. *Arrows* indicate lightly stained tails, and *arrowheads* indicate prominently stained tails. In some stages, KLC3 was also expressed in Sertoli cells in a pattern of streamers. *Scale bars* = 40 μm.

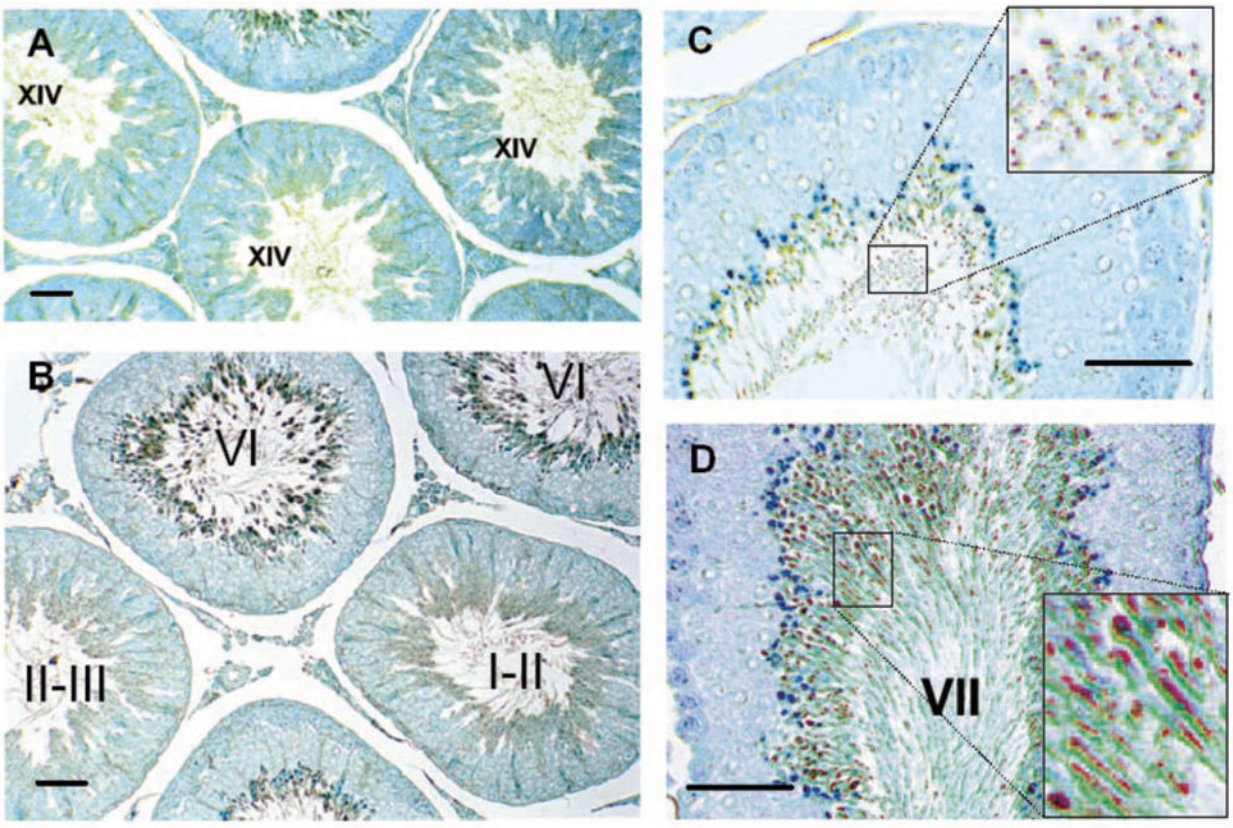

Fig. 3. Immunocytochemistry using monoclonal anti-KLC3 antibodies

Rat testicular sections were analyzed as described in the legend to Fig. 1, except using anti-KLC3 mAb B11. Immunostaining was first observed in the cytoplasm of step 14 spermatids at stage XIV (*A*) and peaked in step 15–16 spermatids at stages I–III (*B*). KLC3 immunostaining could be observed in the midpieces of step 18–19 spermatids in cross-sections (*C*, *inset*) and in longitudinal sections (*D*, *inset*). *Scale bars* = 40 μm.

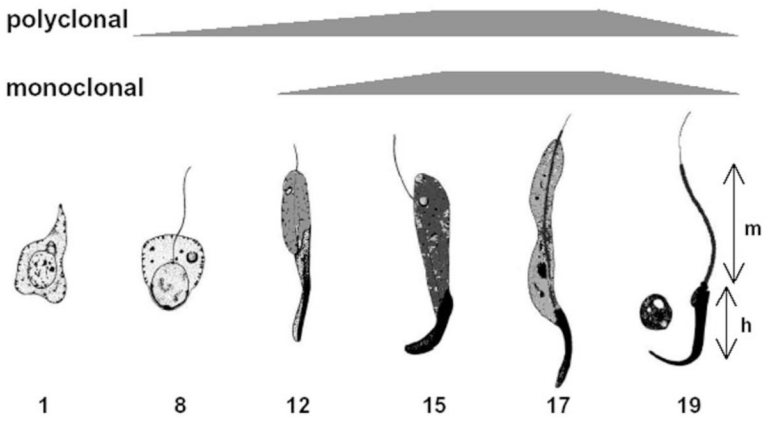

Fig. 4. KLC3 expression during spermiogenesis

Shown are schematic representations of timing (*upper panel*) and pattern of KLC3 expression (*lower panel*) in spermatids during spermiogenesis. Shown are spermatids at different developmental stages ranging from steps 1 to 19 (mature); levels and localization of KLC3 as detected by mAbs are indicated in shades of *gray*. KLC3 is first detected in step 12 spermatids. KLC3 protein accumulates in the midpiece at later stages. The midpiece (*m*) and head (*h*) are indicated.

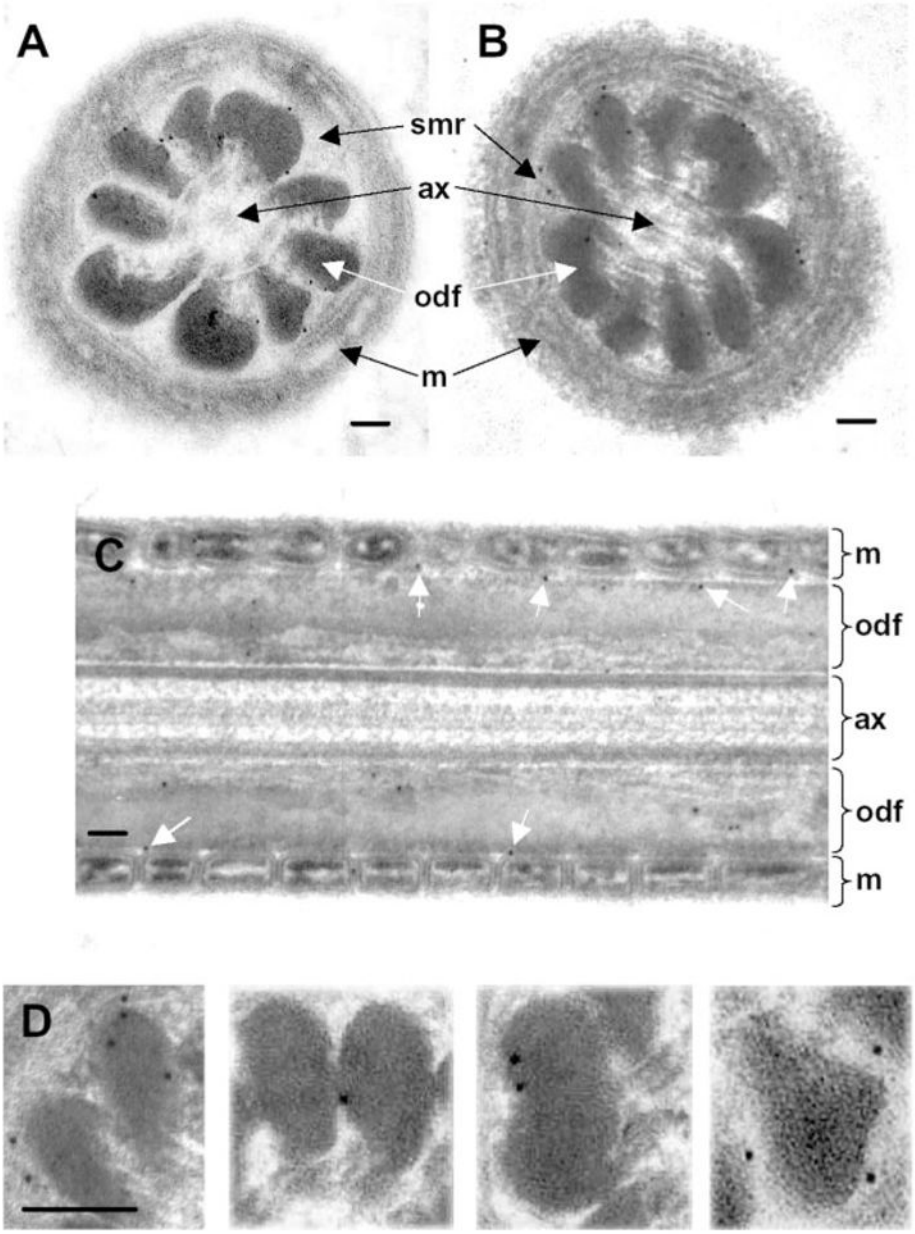

Fig. 5. Immunoelectron microscopic analysis of KLC3 distribution in sperm tails

Ultrastructural analysis of KLC3 localization in sperm tails was carried out using immunogold-labeled anti-KLC3 mAb B11. *A* and *B*, cross-sections through midpieces of mature sperm tails. Note that immunogold label was associated with the surface of ODFs. *C*, longitudinal section through the midpiece of a mature sperm tail. Label was often present between the mitochondrial sheath and the ODFs (*arrows* point to examples). *smr*, submitochondrial reticulum; *ax*, axoneme; *odf*, outer dense fibers; *m*, mitochondria. *D*, examples of gold label in association with ODFs. *Scale bars* = 0.1 μm.

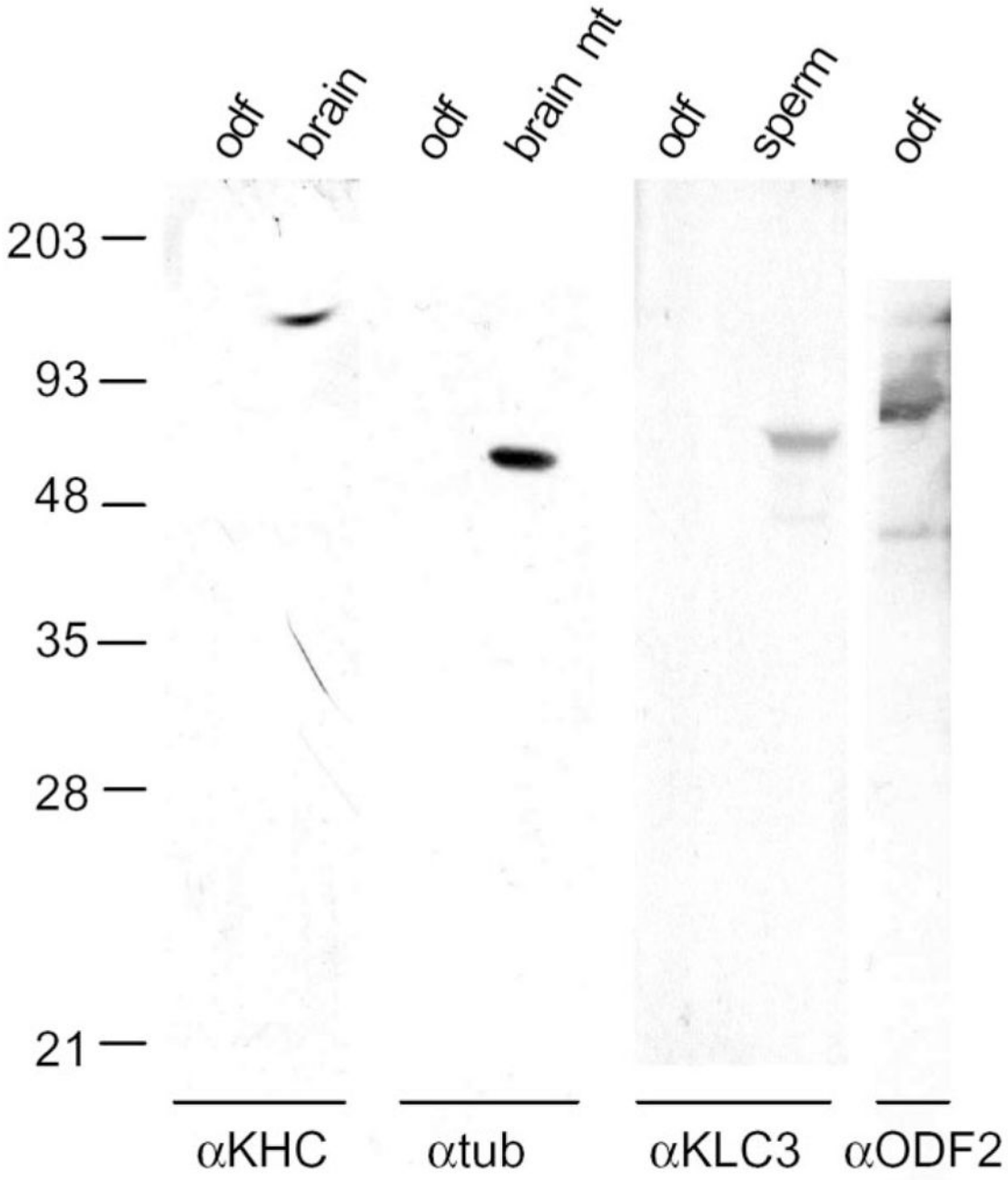

Fig. 6. Purified ODFs do not contain KHC or β-tubulin

To investigate the presence of KHC, β-tubulin, and KLC3 in purified ODF preparations, Western blot analysis was done comparing ODFs with the indicated positive controls. The antisera used in this analysis are indicated below the lanes and include anti-KHC (*αKHC*), anti-β-tubulin (*αtub*), anti-KLC3 (*αKLC3*), and, as positive control for ODF, anti-ODF2 (*αODF2*). *odf*, purified ODFs; *brain*, total brain extract; *brain mt*, purified brain microtubules; *sperm*, sperm tails. Note that ODFs contained ODF2 as expected, but not any of the other proteins analyzed.

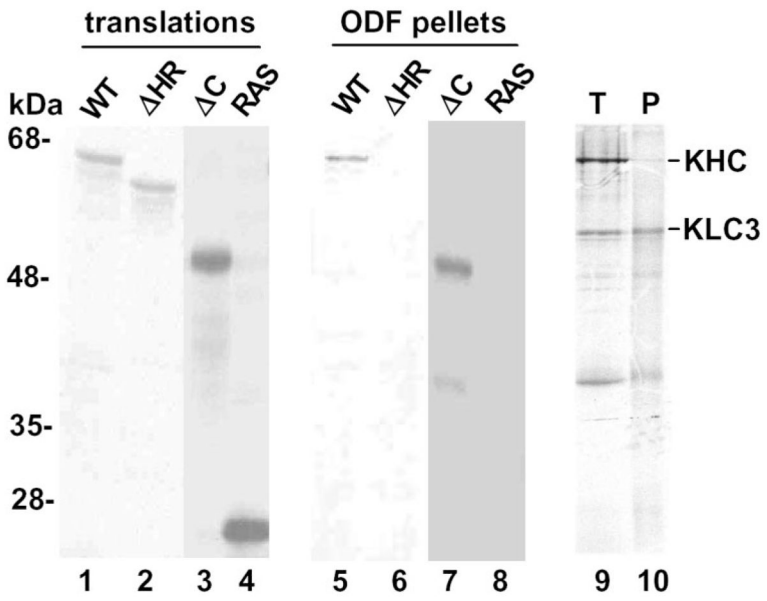

Fig. 7. KLC3 can bind *in vitro* to isolated ODFs

Purified rat ODFs were incubated with *in vitro* translated radiolabeled wild-type KLC3 (*WT*), the KLC3ΔHR mutant (Δ*HR*), the KLC3ΔC mutant (Δ*C*), and p21^{ras} (*RAS*), which was included as a nonspecific control for ODF binding. After repeated washings and pelleting steps, the amount of bound KLC3 in the final pellets was analyzed by SDS-PAGE and autoradiography. *Lanes 1–4* (*translations*) show the input amounts of *in vitro* translated radiolabeled KLC3 variants and p21^{ras} in the different binding reactions. *Lanes 5–8* (*ODF pellets*) show the results from analysis of radiolabeled proteins in the washed ODF pellets. Radiolabeled KLC3 and KHC were mixed and incubated with purified ODFs (*T; lane 9*). Bound protein was analyzed (*P; lane 10*). Note that, whereas wild-type KLC3 and KLC3ΔC bound efficiently to pure ODFs, a mutation in the HR domain (KLC3ΔHR mutant) abolished binding.

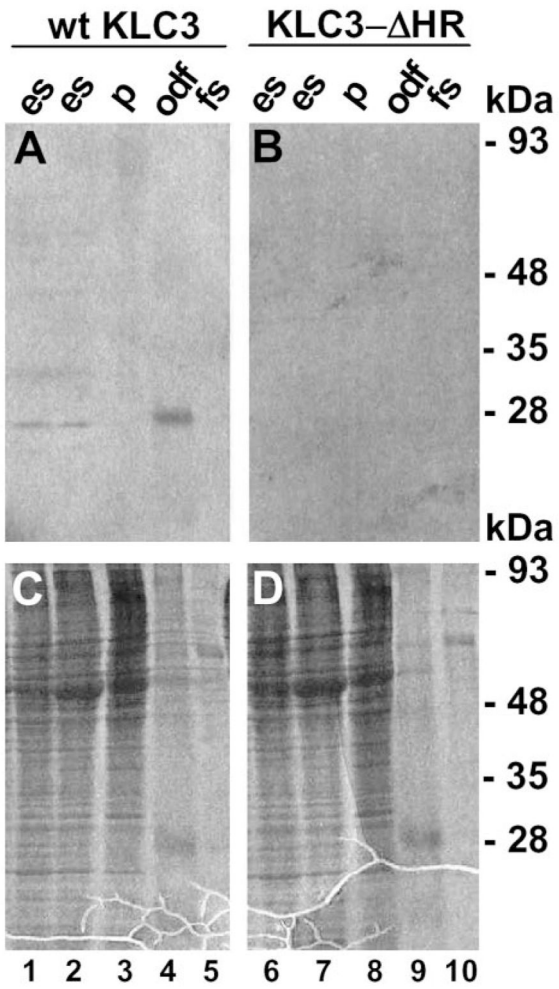

Fig. 8. Interaction of KLC3 with ODF protein

To identify ODF proteins that could associate with KLC3, Western blot overlay experiments were carried out using the indicated radiolabeled proteins (wild-type (*wt*) KLC3 and KLC3ΔHR) as probes. Extracts were prepared from purified early spermatids (*es; lanes 1*, *2*, *6*, and *7*), purified pachytene spermatocytes (*p; lanes 3* and *8*), purified ODFs (*odf; lanes 4* and *9*), and purified FS (*fs; lanes 5* and *10*). Protein extracts were separated by SDS-PAGE, transferred to filters, and incubated with the indicated probes. After washes, filters were exposed. *A* and *B* show autoradiograms of Western blot binding experiments, and *C* and *D* show the corresponding Coomassie staining patterns. Note that the 27-kDa ODF1 protein was present in purified ODF preparations.

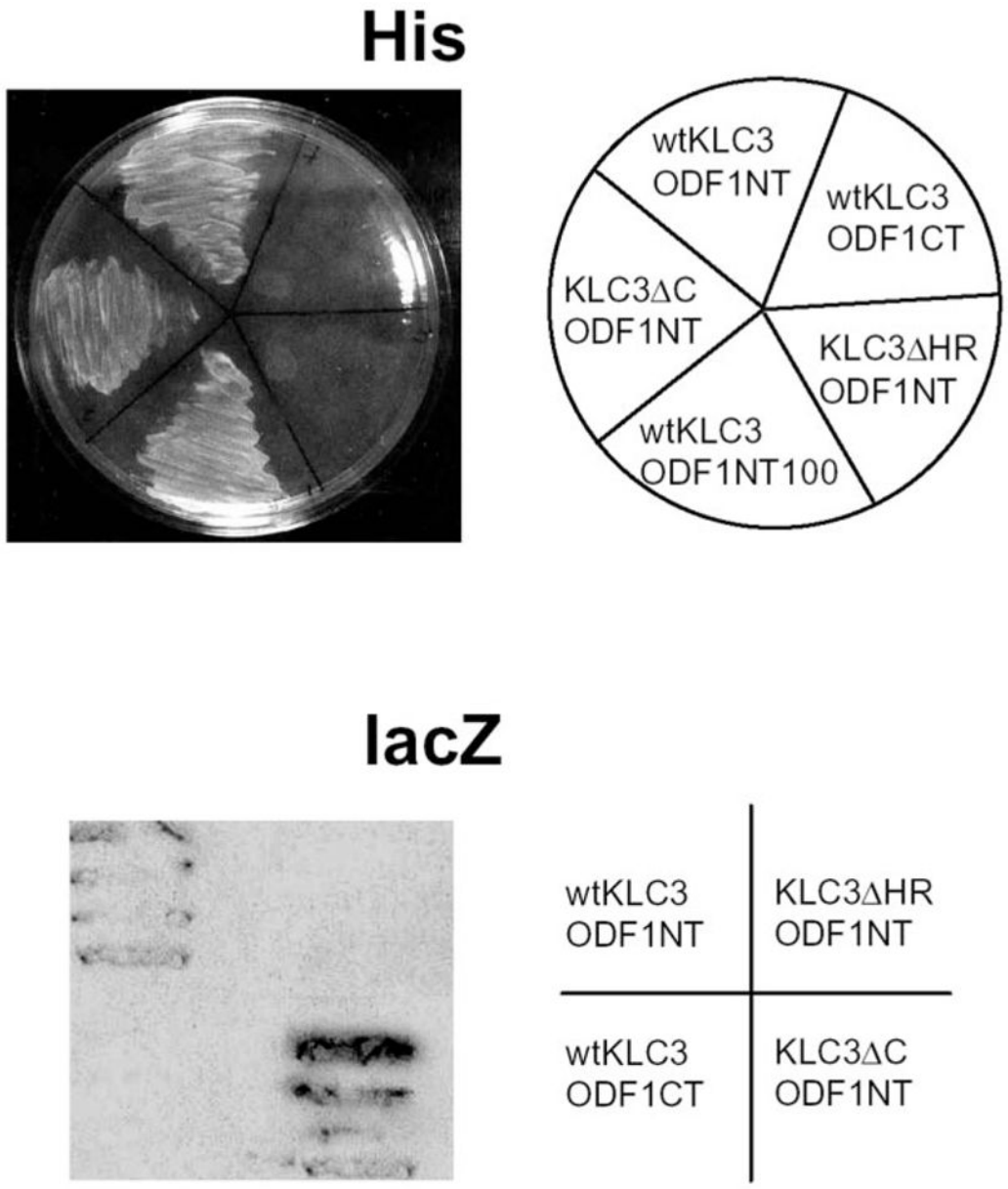

Fig. 9. ODF1 can specifically associate with KLC3 in yeast

The binding of KLC3 to ODF1 was analyzed in yeast. KLC3 expression constructs were based on pGAD424, and ODF1 expression constructs were based on pGBT9 as described previously (20, 29). Growth in the absence of His was tested in yeast strain HF7c (*upper panels*). In His^- growth assays, the plasmid combinations indicated in the *upper right panel* were introduced in yeast strain HF7c, and colonies containing both plasmids were selected and grown as shown in the *upper left panel*. Activation of the *β*-galactosidase reporter gene was tested in yeast strain SFY256 (*lower panels*). For each combination, four yeast SFY256 colonies containing the indicated DNAs were plated as small horizontal streaks, grown, and transferred to filters before carrying out the LacZ assay. ODF1NT and ODF1CT contain the N-and C-terminal halves of ODF1, respectively. *wtKLC3*, wild-type KLC3.

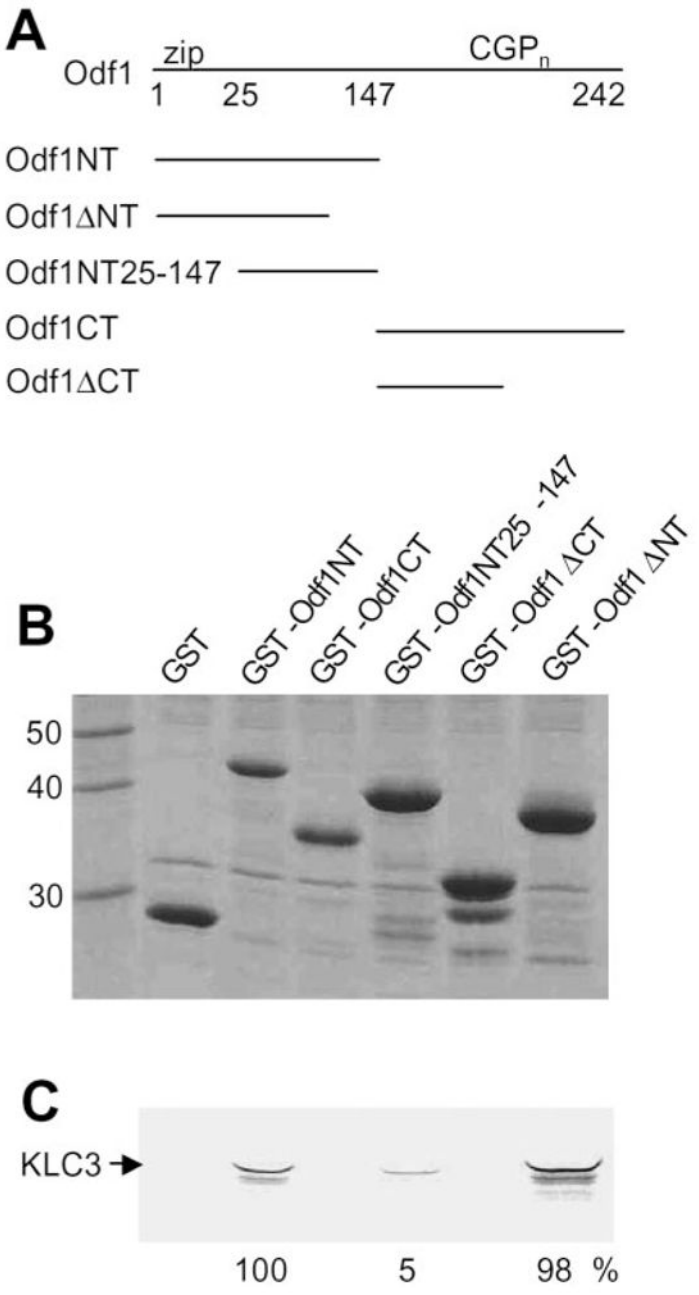

Fig. 10. The ODF1 leucine zipper is involved in KLC3 binding

To analyze ODF1 sequences that mediate binding to the HR domain of KLC3, GST-ODF1 fusion protein pull-down assays were carried out. *A* shows the different ODF1 fragments that were linked to GST and tested for their ability to bind to KLC3. These fusion proteins were expressed in bacteria, purified, and incubated with *in vitro* translated radiolabeled KLC3. *B* shows the fusion proteins used in these experiments after separation by SDS-PAGE and staining with Coomassie. *C* shows the corresponding autoradiogram. The bands in *C* were quantitated and normalized for the different amounts of GST-ODF1 proteins used

in the experiments (see *B*), resulting in the relative binding numbers shown below the autoradiogram (binding to ODF1NT was set arbitrarily at 100%).

Table I

KLC3 binding to ODF1 in yeast

The indicated pGBT and pGAD constructs were tested for protein interaction in the yeast two-hybrid system as described (29).

pGBT construct	pGAD-KLC3	pGAD-KLC3NT	pGAD-KLC3ΔHR	pGAD-KLC3ΔC
ODF1NT[a]	+[b]	+	−	+
ODF1CT[c]	−	−	−	−
ODF1NT100	+	+	ND	ND
ODF2	−	−	ND	ND

[a] ODF1NT contains the N-terminal half of ODF1, which harbors the leucine zipper motif.

[b] +, protein interaction; −, lack of interaction; ND, not determined.

[c] ODF1CT contains the C-terminal half of ODF1, which harbors the conserved CGP repeats.